Chemistry–A European Journal
Research Article
doi.org/10.1002/chem.202201369
Chemistry Europe
European Chemical Societies Publishing
www.chemeurj.org

Direct Comparison of Subvalent, Polycationic Group 13 Cluster Compounds: Lessons learned on Isoelectronic DMPE Substituted Gallium and Indium Tetracation Salts

Antoine Barthélemy,[a] Harald Scherer,[a] and Ingo Krossing*[a]

Dedicated to the occasion of the 60th Birthday of Prof. Cameron Jones.

Abstract: The tetracationic, univalent cluster compounds $[\{M(dmpe)\}_4]^{4+}$ (M = Ga, In; dmpe = *bis*(dimethylphosphino)ethane) were synthesized as their *pf* salts ($[pf]^- = [Al(OR^F)_4]^-$; $R^F = C(CF_3)_3$). The four-membered ring in $[\{M(dmpe)\}_4]^{4+}$ is slightly puckered for M = Ga and almost square planar for M = In. Yet, although structurally similar, only the gallium cluster is prevalent in solution, while the indium cluster forms temperature dependent equilibria that include even the monomeric cation $[In(dmpe)]^+$. This system is the first report of one and the same ligand inducing formation of isoelectronic and isostructural gallium/indium cluster cations. The system allows to study systematically analogies and differences with thermodynamic considerations and bonding analyses, but also to outline perspectives for bond activation using cationic, subvalent group 13 clusters.

Introduction

Subvalent group 13 elements attract increasing interest not only due to their potential in bond activation[1] and catalysis,[2–4] but also due to their rich cluster chemistry. Since group 13 elements M are notoriously electron deficient compounds, the respective ligand supported clusters show a pronounced tendency to accept electrons and thus are often neutral or even anionic.[5–7] Our group demonstrated that the use of a weakly coordinating anion (WCA[8,9]), i.e., $[pf]^-$ ($[pf]^- = [Al(OR^F)_4]^-$; $R^F = C(CF_3)_3$), in combination with weakly coordinating solvents and strongly σ-donating ligands, allowed for formation of cationic, subvalent group 13 clusters.[10,11] On the one hand, the ligands delocalize the positive charge of M^+, thereby minimizing Coulomb repulsion within the cluster, and lift the energy of the ns^2 lone pair, so that these electron pairs can be used to form the M–M bonds within the cluster. On the other hand, the large volume of WCAs thermodynamically favors the formation of highly charged clusters and disfavors disproportionation of metastable M^+ into elemental M^0 and M^{3+}.[10]

Employing this strategy, our group synthesized and isolated tricationic, triangular or tetracationic, rhombohedral In clusters with bipy and phenanthroline,[10] a tetracationic, square planar Ga cluster with ^{t}butylisonitrile[12] (^{t}BuNC) and a pentacationic, pentagonal Ga cluster with DMAP (4-dimethylaminopyridine) as ligands.[13] All of these clusters were obtained using $[M(PhF)_2][pf]$ as the M^+ starting material.[14,15] Interestingly, Ga^+, unlike In^+, disproportionates in the presence of phenanthroline, underlining the differences in the chemistry of subvalent gallium and indium.[12] The stabilizing inert pair effect is more pronounced for the heavier congener, making Ga^+ more prone to disproportionation.[11]

Beyond being chemical curiosities, the cationic gallium and indium clusters $[(ML_m)_x]^{x+}$ (M = Ga, In; L = ligand; $m = 1$ or 2) could possibly be employed in bond activation. Careful ligand design should allow for partial dissociation of the clusters into ligand-supported monomeric species $[:ML_m]^+$ in solution.[13] The metal atom in these fragments possess a ns^2np^0 electron configuration, accounting for their formal carbene[16] or silylene[17]-like character and ambiphilic nature.[11,18,19] Accordingly, it is well known that *neutral* or *anionic* subvalent group 13 complexes efficiently activate covalent bonds.[20]

Since phosphines are electron rich, σ-donating ligands, we rationalized that phosphines may induce cluster formation of univalent gallium and indium cations. Since, most likely, two P-donor atoms have to coordinate to the metal cation in order to promote M–M bond formation, it is crucial to employ a sterically non-demanding phosphine. This is underlined by the fact that $P(^tBu)_3$ and PPh_3 do not induce cluster formation as Ga^+ or In^+ complexes.[14,18] Thus, we assumed that a chelating *bis*phosphine may be a suitable ligand, since ethylene-bridged *bis*phosphines of the type $R_2PCH_2CH_2PR_2$ have generally a smaller Tolman cone angle than two molecules of the respective *mono*phosphines PR_3.[21] As a consequence, we chose

[a] *A. Barthélemy, Dr. H. Scherer, Prof. Dr. I. Krossing*
Institut für Anorganische und Analytische Chemie and
Freiburger Materialforschungszentrum (FMF)
Universität Freiburg
Albertstr. 21, 79104 Freiburg (Germany)
E-mail: krossing@uni-freiburg.de

Supporting information for this article is available on the WWW under https://doi.org/10.1002/chem.202201369

$Me_2PCH_2CH_2PMe_2$ (*bis*(dimethylphosphino)ethane = dmpe) as a model ligand. So far, this *bis*phosphine has allowed for the isolation of unusual transition metal compounds[22] and also of mononuclear group 13 metal complexes[23] but, to the best of our knowledge, has not been employed for the synthesis of main group element clusters.

Results and Discussion

Synthesis

Layering the solutions containing a 1:1 stoichiometric ratio of $[M(PhF)_2][pf]$ (M = Ga, In) and dmpe in *o*DFB with *n*-pentane afforded orange-yellow and dark red crystals of $[\{Ga(dmpe)\}_4][pf]_4 \cdot 4o$DFB ($\mathbf{1}^{4+}([pf]^-)_4 \cdot 4o$DFB) and $[\{In(dmpe)\}_4][pf]_4 \cdot 4o$DFB ($\mathbf{2}^{4+}([pf]^-)_4 \cdot 4o$DFB), respectively, in almost quantitative yields. Both compounds are stable at room temperature (rt), but readily decompose in air. Equation (1) shows their formation and structural formulae.

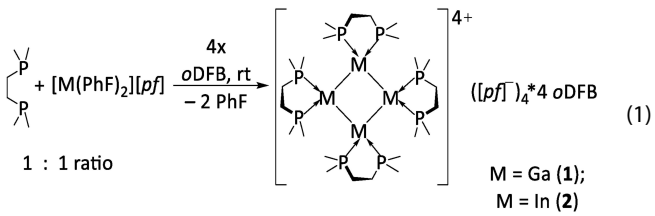

(1)

Molecular structure and bonding

To the best of our knowledge, $\mathbf{1}^{4+}$ and $\mathbf{2}^{4+}$ represent the first two cationic complexes of a chelating *bis*phosphine and subvalent group 13 metal ions. The molecular structure of the cationic clusters as determined by single crystal X-ray analysis is shown in Figure 1, along with selected structural parameters. Apart from $[\{Ga(CN^tBu)\}_4]^{4+}$, the square planar M_4 structure motive has been reported in potassium-stabilized, anionic gallium and indium clusters, i.e., $K_2[Ga_4(C_6H_3\text{-}2,6\text{-}Trip_2)_2]$[24] (Trip = 2,4,6-(^{i}Pr)$_3C_6H_2$)) and $K_2[In_4\{B(NDippCH)_2\}_4]$ (Dipp = 2,6-(^{i}Pr)$_2C_6H_3$)).[7] It is important to note that the alkali–metal counter ions can play a crucial role in stabilizing formally anionic group 13 clusters, which is why they are sometimes rather regarded as mixed alkali–metal-group 13 clusters.[6,7,24,25] By contrast, in the hitherto prepared subvalent cationic clusters, including $\mathbf{1}^{4+}$ and $\mathbf{2}^{4+}$, no M–F_{pf} contact is shorter than the sum of the van-der-Waals radii,[26] indicating that the very weakly coordinating *pf* anion does not interact with the core of the metal atom cluster.[10,12,13]

The average Ga–Ga bond length in $\mathbf{1}^{4+}$ is comparable to those found in $[\{Ga(CN^tBu)\}_4]^{4+}$ (246.1–246.6 pm),[12] $[\{Ga(DMAP)\}_5]^{5+}$ (248.7–250.1 pm),[13] and in the anionic Ga_4 cluster in $K_2[Ga_4(C_6H_3\text{-}2,6\text{-}Trip_2)_2]$ (246.2–246.9 pm).[24] As for the In–In bond lengths in $\mathbf{2}^{4+}$, they are somewhat longer than most of the In–In bonds in the cationic, rhombic bipy- (259.7–280.8 pm) and phenanthroline-supported (258.1–286.1 pm) clusters[10] but similar to those found in the anionic In_4 cluster in $K_2[In_4\{B(NDippCH)_2\}_4]$ (280.5–283.8 pm).[7]

However, it is noteworthy that the average P–M distances (Ga: 237.9–244.8, av. 241.1 pm and In: 259.6–262.4 av. 260.5 pm) are significantly shorter than the average P–M bond lengths in the complexes $[M(PPh_3)_3]^+$ (271_{Ga} and 300_{In} pm) or $[M(P^tBu_3)_2]^+$ (277_{Ga} and 305_{In} pm). The bond shortening can probably be attributed to stronger P–M bonds, since charge delocalization in the clusters is more crucial than in the mononuclear complexes. Consequently, the calculated AIM charge on the M atoms in $\mathbf{1}^{4+}$ and $\mathbf{2}^{4+}$ (0.30 and 0.28 for M = Ga and In; Table 1) is not only reduced compared to the free ions, but also compared to that calculated for the hypothetical monomeric $[M(dmpe)]^+$ fragments (0.50 and 0.56 for M = Ga and In). Remarkably, the P–M distances are only slightly longer than typical P–M^{III} single bond lengths (235_{Ga} and 253_{In} pm).[27]

Interestingly, the In_4 moiety is a nearly perfectly planar square. By contrast, and unlike in the $[\{Ga(CN^tBu)\}_4]^{4+}$ cluster cation, the Ga_4 ring deviates from planarity, with Ga–Ga–Ga–Ga dihedral angles surpassing 20°. Probably, the distortion of the Ga_4 tetragon is caused by steric repulsion of the methyl groups of the dmpe ligands due to the shorter P–M and M–M bonds and thus the smaller M_4 cluster core for M = Ga. However, the two diagonal, transannular Ga–Ga distances [344.8(1) pm and 346.6(1) pm] are considerably longer than the other intramolecular Ga–Ga distances, so that a butterfly structure, which has already been observed in an anionic tetragallanediide,[6] can be ruled out. This is underlined by AIM calculations, which give a ring critical point, but no bond critical point (BCP) in the middle of the Ga_4 moiety (see Section 8.3 in the Supporting Information). The structure of $\mathbf{1}^{4+}$ and $\mathbf{2}^{4+}$ is well reproduced by quantum chemical calculations. Selected calculated structural parameters are compared with experimental parameters in Table 1. Additionally, AIM charges on the M atoms, and bond

Table 1. Calculated structural parameters of $\mathbf{1}^{4+}$ and $\mathbf{2}^{4+}$ (average structural parameters found in the crystal structure are given in parentheses; the average P–M bond lengths and P–M–P bond angles correspond to the values found in the $[M(dmpe)]^+$ subunits. For disordered dmpe ligands, average P–M bond lengths and P–M–P bond angles equate the values found in the majority part of disordered dmpe molecules), along with calculated AIM charges on the metal atoms, bond path ellipticities ε, electron densities on the M–M bond critical points (BCPs) and Wiberg Bond Indices (WBI) of the M–M bonds. Calculations were performed at the RI-BP86(D3BJ)/def2-TZVPP level of theory.

Structural/ Calculated parameters	$\mathbf{1}^{4+}$ (M = Ga)	$\mathbf{2}^{4+}$ (M = In)
M–M bond lengths [pm]	250.7–251.1 (248.5)	291.2 (280.2)
M–M–M angles [°]	88.0–89.0 (88.2)	90.0 (90.0)
M–M–M–M angles [°]	19.3–19.4 (20.4)	0.0 (0)
P–M distances [pm]	242.4–242.7 (241.1)	266.2–267.4 (260.5)
P–M–P angles [°]	85.0–85.2 (84.9)	79.3–79.4 (81.0)
AIM charge on M [e]	0.30	0.28
Bond ellipticity ε on M–M BCPs (average) [a.u.]	0.057	0.037
Electron density on M–M BCPs (average) [e Å^{-3}]	0.403	0.273
WBI of M–M bonds (av.)	0.87	0.74

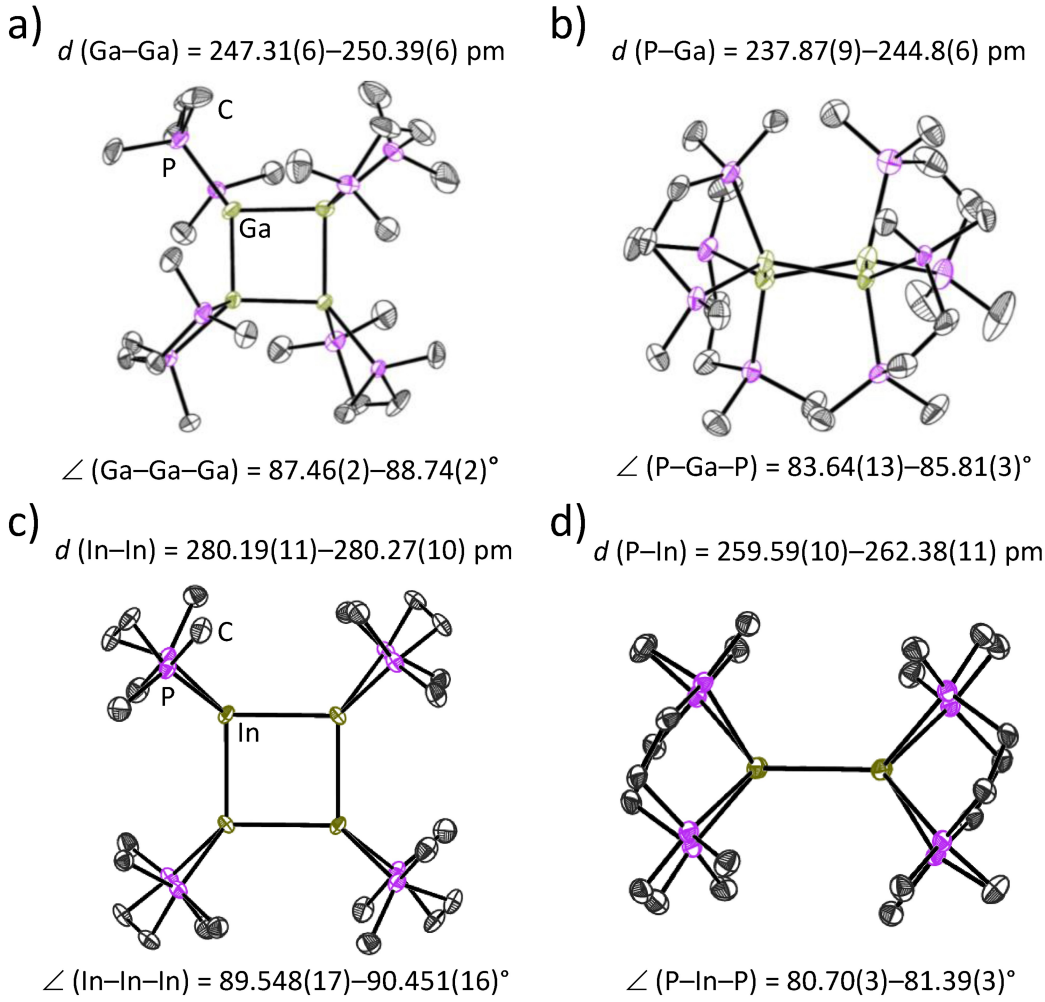

Figure 1. Molecular structures of the cluster cations $\mathbf{1}^{4+}$ (a) and b)) and $\mathbf{2}^{4+}$ (c) and d)). The second perspective is shown in order to visualize the puckered Ga_4 and the planar In_4 ring (M–M–M–M angle: ca. 20.4° for M = Ga and 0° for M = In). Average distances [pm] and angles [°]: Ga–Ga: 248.49(6), P–Ga: 241.1(1), Ga–Ga–Ga: 88.15(2), P–Ga–P: 84.9(1), In–In: 280.2(1), P–In: 260.5(1), In–In–In: 90.00(2), P–In–P: 81.05(3). The P–M bond lengths and P–M–P bond angles correspond to the values found in the $[M(dmpe)]^+$ subunits. For disordered dmpe ligands, the P–M bond lengths and P–M–P bond angles equate the values found in the majority part of disordered dmpe molecules. Counterions, solvent molecules, hydrogen atoms and disordered ligand molecules are not shown for clarity. Thermal ellipsoids are shown at the 50% probability level.

ellipticities as well as electron densities on the M–M bond critical points and Wiberg Bond Indices (WBI) are given.

Both the WBI and the electron density at the M–M BCPs are significantly higher for M = Ga than for M = In, which is indicative of the stronger Ga–Ga bonds compared to the In–In bonds. This agrees with the hypothetical reaction shown in Equation (2),

$$\mathbf{1}^{4+} + 4\,[In(dmpe)]^+ \xrightarrow[\Delta_r G° = +164.1\ kJ\ mol^{-1}]{\Delta_r H° = +171.8\ kJ\ mol^{-1}} \mathbf{2}^{4+} + 4\,[Ga(dmpe)]^+ \quad (2)$$

which is calculated to be endothermic by more than 170 kJ mol^{-1} in the gas phase (RI–BP86(D3BJ)/def2–TZVPP). As a consequence, every Ga–Ga bond in $\mathbf{1}^{4+}$ is inherently stronger than the four In–In bonds in $\mathbf{2}^{4+}$. And this also holds despite the greater steric repulsion of the ligands and greater Coulomb repulsion induced by the shorter Ga–Ga and Ga–P bonds in $\mathbf{1}^{4+}$ if compared to the respective indium system. The smaller HOMO-LUMO gap in the monomeric Ga-unit $[M(dmpe)]^+$ (2.94/3.10 eV for M = Ga/In), qualifies $\mathbf{1}^{4+}$ for better orbital overlap between the monomeric units, hence its HOMO and LUMO. In addition, the frontier orbitals of Ga are less diffuse than for the heavier congener, ensuring better spatial overlap. The frontier orbitals of $\mathbf{1}^{4+}$ and $\mathbf{2}^{4+}$ are depicted in Figure 2.

The HOMO is formed by *p* orbitals, under mixing of the occupied metal *s* orbitals, in the ring plane on the M–M bound edge, while the empty *p* orbitals form a π system perpendicular to the ring plane in the LUMO. The shape of the calculated Kohn-Sham frontier orbitals of $\mathbf{1}^{4+}$ and $\mathbf{2}^{4+}$ are similar, even though the *s-p* mixing in the LUMO of $\mathbf{1}^{4+}$ is more pronounced than in the LUMO of $\mathbf{2}^{4+}$.

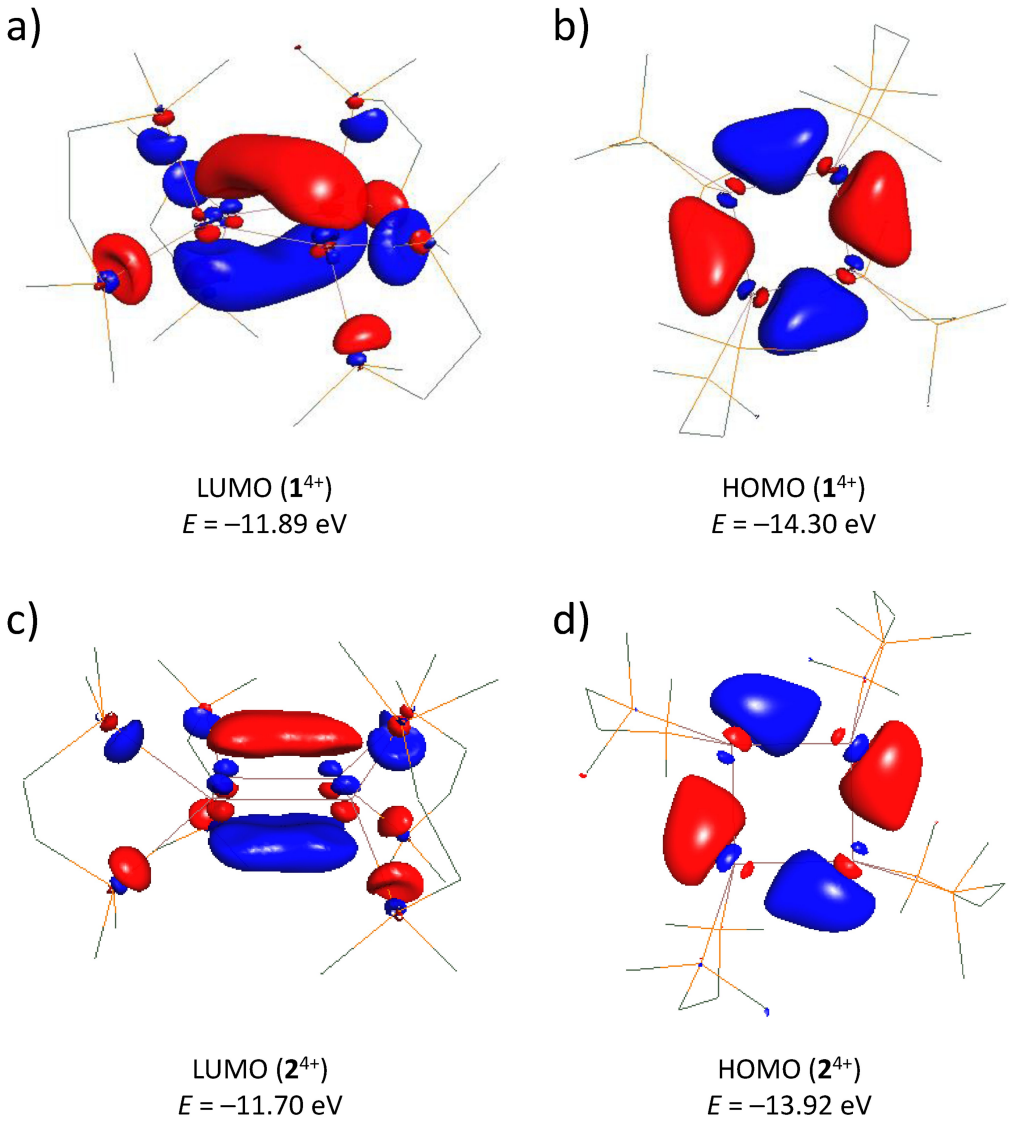

Figure 2. Kohn-Sham frontier orbitals of $\mathbf{1}^{4+}$ (a) LUMO and b) HOMO) and $\mathbf{2}^{4+}$ (c) LUMO and d) HOMO) as well as their energies (RI–BP86(D3BJ)/def2–TZVPP, *iso* value = 0.04).

Clustering in solution and gas phase: DOSY NMR and calculations

NMR spectroscopic measurements confirm that the Ga–Ga bonds are stronger than the In–In bonds in the respective cluster, despite of the weaker Coulomb repulsion in the In_4 cluster with the longer M–M bond lengths: When dissolving crystals of [**1**][*pf*]$_4$·4*o*DFB in *o*DFB, the ^{1}H and ^{31}P NMR spectra suggest that only one dmpe-containing species is present in solution. The ^{1}H chemical shifts of the methylene and the methyl groups are ca. 1.6 and 1.4 ppm downfield, compared to the free ligand in *o*DFB. Similarly, the ^{31}P NMR signal is shifted from −49 ppm for the free ligand to −7 ppm for the Ga^{I}/dmpe complex in *o*DFB (see Section 3.3 in the Supporting Information).

Further results of ^{1}H and ^{19}F diffusion ordered spectroscopy (DOSY) investigations are summarized in Table 2. They show that

Table 2. Diffusion coefficients, ^{1}H and ^{31}P NMR shifts and tentative assignments of different species in *o*DFB solutions of [{M(dmpe)}$_4$][*pf*]$_4$·4*o*DFB (M = Ga, In). Diffusion coefficients were determined with ^{1}H DOSY NMR experiments at rt.

Assignment for [{M(dmpe)}$_x$]$^{x+}$	^{1}H shift [ppm]	^{31}P shift [ppm]	Diffusion coefficient [m^{2}s^{-1}]
M = Ga; x = 4	2.93 and 2.31	−7.1	$(3.285 \pm 0.002) \times 10^{-10}$
M = In; $x \approx 5$	2.88 and 2.28	−16.7	$(2.747 \pm 0.001) \times 10^{-10}$
M = In; $x \approx 4$	2.68 and 2.09	−13.4	$(3.112 \pm 0.001) \times 10^{-10}$
M = In; x = 1	1.83 and 1.27	−7.4	$(8.879 \pm 0.001) \times 10^{-10}$

the diffusion coefficient of the Ga^{I}/dmpe species ($D = (3.285 \pm 0.002) \times 10^{-10}$ m^2/s) is smaller than the diffusion coefficient of the [*pf*]$^-$ anion ($D = (4.737 \pm 0.001) \times 10^{\times 10}$ m^2/s) in the same sample. Hence, the cluster volume has to be larger than that of the [*pf*]$^-$ anion, which agrees well with their thermochemical volumes found in the solid state: from the volume of the [*pf*]$^-$ anion (**727** Å^3),[28] [Ga(*o*DFB)$_2$][*pf*] (971 Å^3),[14] Ga[*pf*] (734 Å^3)[29] and of *o*DFB (**119** Å^3 as calculated from the latter two values) follows that the volume of **1**$^{4+}$ is ca. **1055** Å^3. This clearly implies that the intact cluster **1**$^{4+}$ also exists in solution.

By contrast, three main species were detected via ^{1}H and ^{31}P NMR spectroscopy when dissolving [**2**][*pf*]$_4$·4*o*DFB in *o*DFB. The exact nature of the species corresponding to the low field NMR signals is unclear. However, since these two species display similar, and comparatively low, diffusion coefficients [$D = (2.747 \pm 0.001) \times 10^{-10}$ m^2/s and $(3.112 \pm 0.001) \times 10^{-10}$ m^2/s], we tentatively assign the two signals to In^+/dmpe clusters, for example **2**$^{4+}$, and [{In(dmpe)}$_5$]$^{5+}$. In line with this and according to DFT calculations, the pentamer is only slightly less stable than the tetramer **2**$^{4+}$ in solution (see below).

In agreement with the smaller diffusion coefficients compared to **1**$^{4+}$, **2**$^{4+}$ has a calculated volume of ca. **1150** Å^3 in the solid state, which is slightly greater than the volume of **1**$^{4+}$. The high field ^{1}H NMR signal corresponds to the species with the highest diffusion coefficient ($D = 8.879 \pm 0.001) \times 10^{-10}$ m^2/s). It decreases in intensity upon lowering the temperature and disappears at −20 °C (Figure 3) but increases in intensity, relative to the cluster signals, upon dilution (see Section 3.6 in the Supporting Information). Thus, this signal can probably be assigned to the monomeric [In(dmpe)]$^+$.

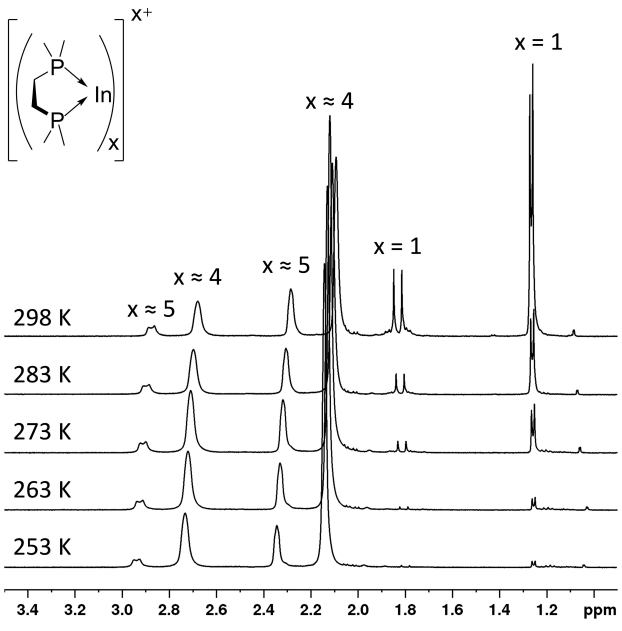

Figure 3. ^{1}H NMR spectra (400.17 MHz, *o*DFB) of crystalline [{In(dmpe)}$_4$][*pf*]$_4$·4*o*DFB measured at 253 K, 263 K, 273 K, 283 K and 298 K (from bottom to top). The signals are tentatively assigned to [In(dmpe)]$^+$, [{In(dmpe)}$_4$]$^{4+}$ and [{In(dmpe)}$_5$]$^{5+}$.

Reactions with excess DMPE

Obviously, the In cluster partly disaggregates in solution, and the position of the dynamic chemical equilibrium between clusters and monomer is altered by temperature change, clearly underlining the weaker M–M bonds in the indium cluster relative to the gallium analogue. Consequently, from solutions of [$In(PhF)_2$][*pf*] and a two-fold excess dmpe, we obtained crystals of the *pf* salt of [In(dmpe)$_2$]$^+$ (see section 6.3 in the Supporting Information). This cation can probably be considered as a trapping product of [In(dmpe)]$^+$ with dmpe and is observed by NMR spectroscopy as the only species in solution in 1:2 mixtures of [$In(PhF)_2$][*pf*] and dmpe. In contrast to this, crystals of [**1**][*pf*]$_4$·4*o*DFB are reproducibly isolated from [Ga(PhF)$_2$][*pf*]/dmpe mixtures, even when employing a two-fold excess of dmpe. Additionally, in solutions of Ga^+ and excess dmpe, the cluster **1**$^{4+}$ is still detected and decreases only very slowly over weeks. Since the formation of [M(dmpe)$_2$]$^+$ from dmpe and **1**$^{4+}$ or **2**$^{4+}$ is thermodynamically favorable for both M_4 clusters in *o*DFB ($\Delta_r G^\circ_{oDFB} = -81$ and -207 kJ mol^{-1} for **1**$^{4+}$ and **2**$^{4+}$, respectively; RI–BP86(D3BJ)/def2–TZVPP), these findings underline that **1**$^{4+}$ is not only thermodynamically, but also kinetically more stable than **2**$^{4+}$.

Thermodynamics of disaggregation

The different dissociation tendencies of both clusters as shown in Equation (3) are well described by DFT calculations.

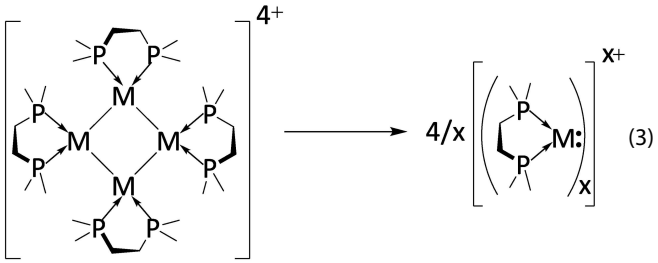

(3)

Hence, Table 3 delineates that the dissociation of **gaseous** [{M(dmpe)}$_4$]$^{4+}$ is always both, highly exothermic and exergonic

Table 3. Calculated standard Gibbs free energies and enthalpies for the dissociation of **1**$^{4+}$ and **2**$^{4+}$ into mono- or oligomeric [{M(dmpe)}$_x$]$^{x+}$ according to Equation (3) in the gas phase and an *o*DFB solution at 298 K ($\varepsilon_r = 13.38$;[30] COSMO model, RI-BP86(D3BJ)/def2-TZVPP). Note that the formation of the dimer is less favored than the formation of the higher clusters, due to the presence of a non-classical, double dative double bond, which is weaker than the σ bonds in the higher cluster compounds (see Sections 8.5 and 8.7.15 in the Supporting Information).[31]

Product Complex	$\Delta_r H^\circ$ (gas) [kJ mol^{-1}]	$\Delta_r G^\circ$ (gas) [kJ mol^{-1}]	$\Delta_r G^\circ$ (*o*DFB) [kJ mol^{-1}]
M = Ga; $x = 1$	−576.2	−745.7	+193.8
M = In; $x = 1$	−748.0	−909.8	−12.5
M = In; $x = 2$	−469.1	−562.5	+33.7
M = In; $x = 3$	−224.2	−257.8	+19.4
M = In; $x = 5$	+241.4	+254.8	+6.2
M = In; $x = 6$	+485.1	+508.2	+8.4

for $x=1$ by several hundred kJ mol^{-1}. This is a consequence of the reduction of the charge from 4+ to 1+ in a Coulomb explosion. In addition, the clear preference for the monocation over the clustered cations in the gas phase underlines the crucial role of the highly polar, but non-basic *o*DFB-solvent with $\varepsilon_r = 13.38$[30] to stabilize multiply charged cluster ions. While the dissociation of $\mathbf{1}^{4+}$ to the monomer is endergonic by almost +200 kJ mol^{-1} in an *o*DFB solution, the dissociation of $\mathbf{2}^{4+}$ is nearly thermoneutral in $\Delta_r G^\circ$. Hence, it agrees well with the temperature dependence of the signal assigned to the monomer with $x=1$ observed by NMR.

From the NMR spectra it is noticeable that the concentration of the pentamer is barely affected by temperature variations (see Figure 3 and Table S2 in the Supporting Information). However, the concentration of this cluster increases slowly over time at rt, decreases disproportionately upon dilution and the $^1H\{^{31}P\}$ EXSY NMR shows a weak correlation between this species and the monomer (see Section 3.6.1 in the Supporting Information). These findings indicate that the pentamer is in chemical exchange with the other two species, but that its formation is kinetically hindered. Under the assumption that the formation of this complex is too slow to significantly affect the equilibrium between the two other species and that the three species are indeed monomeric, tetrameric and pentameric, a van't Hoff analysis was performed in order to determine $\Delta_r H^\circ$, $\Delta_r S^\circ$ and $\Delta_r G^\circ$ for the tetramer-monomer conversion experimentally (see Section 3.6.2 in the Supporting Information).[1] The results are summarized in Table 4.

Evidently, due to the assumptions made, care must be taken when interpreting the exact values. However, the good linear correlation found in the van't Hoff plot ($R^2=0.98$) indicates that the two involved species may indeed be a tetrameric cluster and a monomer. According to the van't Hoff analysis, the dissociation of the cluster into the monomer is endothermic and entropically favored. Besides, these thermodynamics rationalize well the observed shift of the chemical equilibrium towards the putative tetramer upon temperature reduction. Most importantly, the obtained thermodynamics suggest that the dissociation of the In–dmpe cluster tetramer into the monomer is nearly thermoneutral at rt in *o*DFB and the experimental value (+21.3 ± 24.2 kJ mol^{-1}, Table 4) agrees within 1.3 σ with the quantum chemical calculation in Table 3 (−12.5 kJ mol^{-1}).

Table 4. Experimentally determined reaction enthalpy, entropy and Gibbs free energy for the tetramer-monomer conversion by means of a van't Hoff analysis of the variable temperature NMR spectra in *o*DFB.

Reaction	$\Delta_r H^\circ$ [kJ mol^{-1}]	$\Delta_r S^\circ$ [J K^{-1} mol^{-1}]	$\Delta_r G^\circ$ [kJ mol^{-1}]
$[\{In(dmpe)\}_4]^{4+}{}_{(solv)} \rightarrow 4\ [In(dmpe)]^{+}{}_{(solv)}$	220.6 ± 16.3	668.6 ± 59.9	21.3 ± 24.2

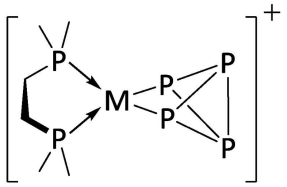

Figure 4. Proposed structure of the hypothetical insertion product of monomeric $[:M(dmpe)]^+$ in a P–P bond of P_4.

Reactions with P_4

The notion that $\mathbf{1}^{4+}$ exists exclusively as tetramer in solution, but $\mathbf{2}^{4+}$ dissociates with monomer formation is further supported by two reactions of $\mathbf{1}^{4+}$ and $\mathbf{2}^{4+}$ with one equivalent of P_4 in *o*DFB each. Quantum chemical calculations suggest that the monomeric $[:Ga(dmpe)]^+$ fragment should insert in an exergonic reaction ($\Delta_r G^\circ{}_{oDFB} = -71$ kJ mol^{-1}) and with a low activation energy of $\Delta G^{\circ\neq}{}_{oDFB} = 57$ kJ mol^{-1} into a P–P bond of P_4, yielding a complex as shown in Figure 4 with M = Ga.

Related complexes with η^2-coordinated or truly inserted P_4 molecules have already been reported for several metal atoms,[32] including subvalent gallium.[33] By contrast, the reaction of the respective In monomer is endergonic both in the gas phase and in *o*DFB ($\Delta_r G^\circ{}_{oDFB} = +14$ kJ mol^{-1}) and has a considerably higher activation energy of $\Delta G^{\circ\neq}{}_{oDFB} = 104$ kJ mol^{-1}. The energy profiles for the reaction in an *o*DFB solution are depicted in Scheme 1 and illustrate well the greater bond activating potential of cationic gallylene $[:Ga(dmpe)]^+$ compared to the analogous indylene $[:In(dmpe)]^+$. The calculated structures of the monomeric $[:M(dmpe)]^+$ ($\mathbf{A}_M$) species, the complexes with loosely bound P_4 ($\mathbf{B}_M$) as well as the P–P insertion products ($\mathbf{C}_M$) and the corresponding transition states **TS** $\mathbf{B}_M/\mathbf{C}_M$ (M = Ga or In) are also included. Since the structures are very similar for both metal cations, only the optimized structures for M = Ga are shown.

The outcome of the reactions for both cationic clusters is summarized in Equations (4) and (5). In agreement with the expectation, **no** reaction occurs upon mixing of $[\mathbf{1}][pf]_4 \cdot 4o$DFB with P_4 in *o*DFB even at 60 °C.

$$\mathbf{1}^{4+} + P_4 \xrightarrow{o\text{DFB, 60 °C}} \text{no reaction} \quad (4)$$

$$\mathbf{2}^{4+} + P_4 \xrightarrow{o\text{DFB, 60 °C}} \left[\text{P}_3\right]^+ + ? \quad (5)$$

Hence, **no** substantial amounts of the monomer appear in an equilibrium in solution, in line with the results of the thermodynamic calculations (cf. Table 3). By contrast, a mixture

[1] It was also observed that $[\mathbf{2}][pf]_4 \cdot 4\ C_6H_4F_2$ partly decomposes in solution and that a small amount of a precipitate, consisting of elemental indium and other crystalline and amorphous compounds, formed, which adds uncertainty to the exact concentration of the three species. For the van't Hoff analysis of this system, it was postulated that for the time the measurements took, these decomposition reactions do not affect the result of the analysis significantly. See Section 3.6 in the Supporting Information for a detailed discussion of the decomposition reactions.

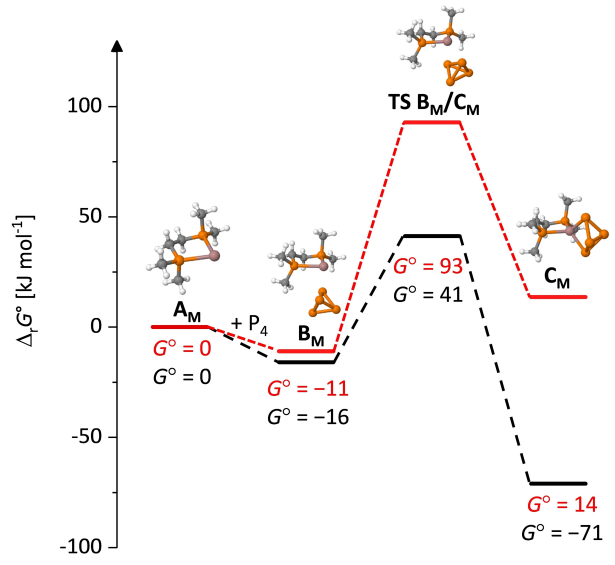

Scheme 1. Energy profiles for the P_4 activation with $[:In(dmpe)]^+$ (red; M = In) and $[:Ga(dmpe)]^+$ (black; M = Ga) in an *o*DFB solution. In the gas phase, slightly higher activation barriers $\Delta G^{\circ\neq}$ are calculated (67 kJ mol^{-1} for M = Ga and 119 kJ mol^{-1} for M = In; see Section 8.6 in the Supporting Information). The optimized molecular structures of the intermediates $\mathbf{A_M}$, $\mathbf{B_M}$ and $\mathbf{C_M}$ and for the transition state **TS** $\mathbf{B_M/C_M}$ are included ($\varepsilon_r = 13.38$;[30] COSMO model, RI–BP86(D3BJ)/def2–TZVPP). Only the optimized structures for M = Ga are shown.

of products formed in the reaction of P_4 with $[\mathbf{2}][pf]_4 \cdot 4o$DFB, however, **no** P–P insertion products like $[(dmpe)InP_4]^+$ were detected, again in accordance with the DFT calculations. Unexpectedly, we found that the main product of this reaction is $[(Me_2PCH_2CH_2PMe_2)P]^+$, i.e., a five-membered, cyclic triphosphenium cation [see Equation (5) and Section 3.7 in the Supporting Information].[34] The formation of this product suggests that, under these reaction conditions, In^+ acts as an oxidizing agent towards P_4, possibly initiated from the accessible complex $\mathbf{B_{In}}$ in Scheme 1. The oxidizing behaviour of cationic, subvalent gallium in non-coordinating environments towards silanes was recently demonstrated as being higher than that of the ferrocenium ion.[3] These findings again underline that carbenoid-like monomers of the type $[L_2M:]^+$ display interesting reactivity, and, after careful ligand design, may be employed in bond activation reactions.

Conclusion

We synthesized and characterized two novel, cationic clusters of subvalent gallium and indium by employing the weakly coordinating $[pf]^-$ anion and the chelating, electron rich dmpe ligand. The salts $[\{M(dmpe)\}_4][pf]_4 \cdot 4o$DFB (M = Ga, In) represent the first phosphine-supported cationic gallium and indium clusters to be isolated and the first cationic complexes of a *bis*phosphine and subvalent group 13 metal cations to be reported. For the first time, we observed that one and the same ligand induces formation of isoelectronic, cationic gallium and indium clusters, allowing to directly compare the M–M bonding situation. The indium cluster forms a nearly perfect square in the solid-state structure, whereas the gallium analogue is slightly puckered and deviates from planarity, which is attributed to the greater steric repulsion of the ligands in the stronger metal–metal bound gallium cluster. We also investigated the stability of the two clusters in solution both by quantum chemical calculations and experimentally. NMR measurements reveal that the Ga cluster does not dissociate in an *o*DFB solution at rt, unlike the In congener. This agrees with the stronger Ga–Ga compared to In–In bonds. The bond activation of P_4, calculated to be thermodynamically and kinetically feasible with the Ga^I monomer, was absent in solutions with the Ga cluster. Hence, the monomer is not available in equilibrium, only the clustered tetracation $\mathbf{1}^{4+}$. Similarly, the reaction with P_4 was unfavorable for the In^I system, which dissociates in equilibrium to the monomer in solution. But here the thermodynamic driving force to insertion was insufficient. Thus, the focus in this research field will lie on designing and fine-tuning ligands for subvalent group 13 cluster cations that induce either formation of stable clusters or that of labile, catalytically active clusters, which partly dissociate in equilibrium in solution, providing the catalytically active monomer. Our herein presented study suggests that chelating phosphines may be well suited ligands to induce this reactivity. Overall, catalysis involving a cycle including oxidative addition and reductive elimination at a subvalent group 13 metal centre is particularly promising for Ga^+, as Wehmschulte already showed that reductive elimination is facilitated at this element.[4]

Experimental Section

All manipulations were carried out under exclusion of moisture and air through usage of a MBraun glovebox filled with nitrogen (O_2/H_2O < 1 ppm) and standard Schlenk techniques. All glassware used in reactions have been stored overnight in an oven at 180 °C and were additionally dried with a heat gun prior to use. All solvents were stored under an atmosphere of argon or nitrogen in sealed vessels. Fluorobenzene and *ortho*-difluorobenzene (*o*DFB) were dried over CaH_2 for two days, distilled and degassed prior to use. The water content of the solvents was below 10 ppm, as determined by Karl Fischer titration. *Bis*(dimethylphosphino)ethane (dmpe) was used as received. Li[*pf*] ($[pf]^- = [Al(OR^F)_4]^-$, $R^F = C(CF_3)_3$),[8] Ag[*pf*],[8,35] $[Ga(PhF)_2][pf]$[14] and $[In(PhF)_2][pf]$[18] were prepared according to literature protocols. Note that the number of fluorobenzene molecules coordinated to M^+ in $[M(PhF)_2][pf]$ (M = Ga, In) can vary, depending on the vacuum applied when drying the product. Thus, the formula $[M(PhF)_2][pf]$ is used for the sake of simplicity instead of $[M(PhF)_x][pf]$ ($1 < x < 3$). The exact ratio x was determined via ^{19}F NMR spectroscopy.

Synthesis of $[\mathbf{1}][pf]_4 \cdot 4\,C_6H_4F_2$: Layering a solution of dmpe (0.225 M in *o*DFB, 0.8 mL, 180 µmol) and $[Ga(PhF)_1][pf]$ (204 mg, 180 µmol, 1.0 equiv.) with pentane at rt or with heptane at −25 °C (ca. 8 mL, respectively) afforded yellow-orange crystals after 1 d. After removal of the solvent, crystalline $[\mathbf{1}][pf]_4 \cdot 4\,C_6H_4F_2$ was obtained in very good yield (214 mg, 164 µmol, 91 %). Employing a two-fold excess of dmpe also yielded crystals of $[\mathbf{1}][pf]_4 \cdot 4\,C_6H_4F_2$. ^1H NMR [400.17 MHz, *o*DFB, 298 K]: $\delta = 2.93$ (m, 16 H, CH_2), 2.31 (m, 48 H, CH_3) ppm. $^{13}C\{^1H\}$ NMR [100.62 MHz, *o*DFB, 298 K]: $\delta = 24.5$ (8 C, CH_2), 12.4 (16 C, CH_3) ppm. ^{19}F NMR [376.54 MHz, *o*DFB, 298 K]: $\delta = -75.3$ (s, 36 F, $[Al(OC(CF_3)_3)_4]^-$) ppm. ^{27}Al NMR [104.27 MHz,

*o*DFB, 298 K]: $\delta = 35.0$ (1 Al, [**Al**$(OC(CF_3)_3)_4]^-$) ppm. $^{31}P\{^1H\}$ NMR [161.99 MHz, *o*DFB, 298 K]: $\delta = -7.1$ (8 P) ppm. ^{71}Ga NMR [122.04 MHz, *o*DFB, 298 K]: signal probably too broad to be detected, due to the quadrupolar relaxation of ^{71}Ga.

Synthesis of [2][*pf*]$_4$·4 $C_6H_4F_2$: Layering a solution of dmpe (0.225 M in oDFB, 0.8 mL, 180 μmol) and [In(PhF)$_1$][*pf*] (212 mg, 180 μmol, 1.0 equiv.) with pentane at rt or with heptane at −25 °C (ca. 8 mL, respectively) afforded dark red crystals after 1 d. After removal of the solvent, crystalline [**2**][*pf*]$_4$·4 $C_6H_4F_2$ was obtained in very good yield (223 mg, 166 μmol, 92%). ^1H NMR [400.17 MHz, *o*DFB, 298 K]: $\delta = 2.88$ (m, 20 H, C**H**$_2$, $x \approx 5$), 2.68 (m, 16 H, C**H**$_2$, $x \approx 4$), 2.28 (m, 60 H, C**H**$_3$, $x \approx 5$), 2.09 (m, 48 H, C**H**$_3$, $x \approx 4$), 1.83 (m, 4 H, C**H**$_2$, $x = 1$), 1.27 (m, 12 H, C**H**$_3$, $x = 1$) ppm. $^{13}C\{^1H\}$ NMR [100.62 MHz, *o*DFB, 298 K]: $\delta = 26.0$ (2 C, $x = 1$, **C**H$_2$), 25.5 (10 C, $x \approx 5$, **C**H$_2$), 25.1 (8 C, $x \approx 4$, **C**H$_2$), 12.8 (20 C, $x \approx 5$, **C**H$_3$), 12.5 (16 C, $x \approx 4$, **C**H$_3$), 8.3 (4 C, $x = 1$, **C**H$_3$) ppm. ^{19}F NMR [376.54 MHz, *o*DFB, 298 K]: $\delta = -75.3$ [s, 36 F, [Al(OC(C**F**$_3)_3)_4]^-$] ppm. ^{27}Al NMR [104.27 MHz, *o*DFB, 298 K]: $\delta = 35.0$ (1 Al, [**Al**$(OC(CF_3)_3)_4]^-$) ppm. $^{31}P\{^1H\}$ NMR [161.99 MHz, *o*DFB, 298 K]: $\delta = -7.4$ (2 P, $x = 1$), −13.4 (8 P, $x \approx 4$), −16.7 (10 P, $x \approx 5$) ppm. ^{115}In NMR [122.04 MHz, *o*DFB, 298 K]: $\delta = -1324$ (br., 1 In, [**In**(fluoroarene)$_x]^+$; $\nu_{1/2} = 3300$ Hz) ppm.

Synthesis of [In(dmpe)$_2$][*pf*]: Layering a solution of dmpe (0.225 M in *o*DFB, 0.76 mL, 171 μmol, 2.0 equiv.) and [In(PhF)$_1$][*pf*] (101 mg, 86 μmol, 1.0 equiv.) with pentane at rt or with heptane at −25 °C (ca. 8 mL, respectively) afforded beige crystals after 1 d. After removal of the solvent, crystalline [In(dmpe)$_2$][*pf*] was obtained in good yield (97 mg, 70 μmol, 82%).^1H NMR [300.18 MHz, *o*DFB, 298 K]: $\delta = 1.64$ (m, 8 H, C**H**$_2$), 1.17 (m, 24 H, C**H**$_3$) ppm. $^{13}C\{^1H\}$ NMR [75.48 MHz, *o*DFB, 298 K]: $\delta = 26.6$ (4 C, **C**H$_2$), 11.8 (8 C, **C**H$_3$) ppm. ^{19}F NMR [282.45 MHz, *o*DFB, 298 K]: $\delta = -75.3$ (s, 36 F, [Al(OC-(C**F**$_3)_3)_4]^-$) ppm. ^{27}Al NMR [78.22 MHz, *o*DFB, 298 K]: $\delta = 35.0$ (1 Al, [**Al**$(OC(CF_3)_3)_4]^-$) ppm. $^{31}P\{^1H\}$ NMR [121.52 MHz, *o*DFB, 298 K]: $\delta = -35.5$ (4 P) ppm. ^{115}In NMR [65.78 MHz, *o*DFB, 298 K]: signal probably too broad to be detected, due to the quadrupolar relaxation of ^{115}In.

Deposition Numbers 2157680 (for [**1**][*pf*]$_4$·4 $C_6H_4F_2$), 2157681 (for [**2**][*pf*]$_4$·4 $C_6H_4F_2$), 2157682 (for [In(dmpe)$_2$][*pf*]) contain the supplementary crystallographic data for this paper. These data are provided free of charge by the joint Cambridge Crystallographic Data Centre and Fachinformationszentrum Karlsruhe Access Structures service.

Acknowledgements

This work was supported by the Albert-Ludwigs-Universität Freiburg and by the DFG in the Normalverfahren. We would like to thank Dr. Harald Scherer and Fadime Bitgül for the measurement of the NMR spectra, Dr. Thilo Ludwig and Dr. Michael Daub for the collection of the powder XRD data and Dr. Burkhard Butschke for his support regarding single X-ray crystallography. The authors acknowledge support by the state of Baden-Württemberg through bwHPC and the German Research Foundation (DFG) through grant no. INST 40/467-1 and 575-1 FUGG (JUSTUS1 and 2 cluster). A. B. thanks the "Fonds der Chemischen Industrie" for a Ph.D. fellowship. Open Access funding enabled and organized by Projekt DEAL.

Conflict of Interest

The authors declare no conflict of interest.

Keywords: DFT · main group chemistry · polycationic gallium and indium clusters · subvalent group 13 elements · weakly coordinating anion (WCA)

[1] a) C. Jones, D. P. Mills, R. P. Rose, *J. Organomet. Chem.* **2006**, *691*, 3060; b) A. Seifert, D. Scheid, G. Linti, T. Zessin, *Chem. Eur. J.* **2009**, *15*, 12114; c) T. Chu, I. Korobkov, G. I. Nikonov, *J. Am. Chem. Soc.* **2014**, *136*, 9195; d) C. Ganesamoorthy, D. Bläser, C. Wölper, S. Schulz, *Organometallics* **2015**, *34*, 2991; e) J. Hicks, P. Vasko, J. M. Goicoechea, S. Aldridge, *Nature* **2018**, *557*, 92; f) M. Schorpp, R. Tamim, I. Krossing, *Dalton Trans.* **2021**, *50*, 15103; g) K. Koshino, R. Kinjo, *J. Am. Chem. Soc.* **2021**, *143*, 18172.
[2] a) M. R. Lichtenthaler, A. Higelin, A. Kraft, S. Hughes, A. Steffani, D. A. Plattner, J. M. Slattery, I. Krossing, *Organometallics* **2013**, *32*, 6725; b) M. R. Lichtenthaler, S. Maurer, R. J. Mangan, F. Stahl, F. Mönkemeyer, J. Hamann, I. Krossing, *Chem. Eur. J.* **2015**, *21*, 157; c) B. Qin, U. Schneider, *J. Am. Chem. Soc.* **2016**, *138*, 13119; d) S. Dagorne, R. Wehmschulte, *ChemCatChem* **2018**, *10*, 2509; e) Z. Li, G. Thiery, M. R. Lichtenthaler, R. Guillot, I. Krossing, V. Gandon, C. Bour, *Adv. Synth. Catal.* **2018**, *360*, 544; f) C. Weetman, S. Inoue, *ChemCatChem* **2018**, *10*, 4213; g) H.-J. Jung, Y. Cho, D. Kim, P. Mehrkhodavandi, *Catal. Sci. Technol.* **2021**, *11*, 62.
[3] A. Barthélemy, K. Glootz, H. Scherer, A. Hanske, I. Krossing, *Chem. Sci.* **2022**, *13*, 439.
[4] R. J. Wehmschulte, R. Peverati, D. R. Powell, *Inorg. Chem.* **2019**, *58*, 12441.
[5] a) O. T. Beachley, R. Blom, M. R. Churchill, K. Faegri, J. C. Fettinger, J. C. Pazik, L. Victoriano, *Organometallics* **1989**, *8*, 346; b) W. Uhl, W. Hiller, M. Layh, W. Schwarz, *Angew. Chem. Int. Ed.* **1992**, *31*, 1364; c) R. D. Schluter, A. H. Cowley, D. A. Atwood, R. A. Jones, J. L. Atwood, *J. Coord. Chem.* **1993**, *30*, 25; d) P. J. Brothers, K. Hübler, U. Hübler, B. C. Noll, M. M. Olmstead, P. P. Power, *Angew. Chem. Int. Ed.* **1996**, *35*, 2355; e) W. Uhl, A. Jantschak, W. Saak, M. Kaupp, R. Wartchow, *Organometallics* **1998**, *17*, 5009; f) N. Wiberg, *J. Organomet. Chem.* **1999**, *574*, 246; g) N. Wiberg, T. Blank, H. Nöth, W. Ponikwar, *Angew. Chem. Int. Ed.* **1999**, *38*, 839; h) N. Wiberg, T. Blank, A. Purath, G. Stößer, H. Schnöckel, *Angew. Chem. Int. Ed.* **1999**, *38*, 2563; i) A. Schnepf, G. Stößer, R. Köppe, H. Schnöckel, *Angew. Chem. Int. Ed.* **2000**, *39*, 1637; j) A. Schnepf, G. Stösser, H. Schnöckel, *J. Am. Chem. Soc.* **2000**, *122*, 9178; k) A. Schnepf, H. Schnöckel, *Angew. Chem. Int. Ed.* **2001**, *40*, 711; l) A. Schnepf, G. Stößer, H. Schnöckel, *Angew. Chem. Int. Ed.* **2002**, *41*, 1882; m) A. Donchev, A. Schnepf, E. Baum, G. Stößer, H. Schnöckel, *Z. Anorg. Allg. Chem.* **2002**, *628*, 157; n) G. Linti, A. Seifert, *Dalton Trans.* **2008**, 3688; o) M. Gast, B. Ejlli, H. Wadepohl, G. Linti, *Eur. J. Inorg. Chem.* **2019**, *2019*, 2964.
[6] N. Wiberg, T. Blank, M. Westerhausen, S. Schneiderbauer, H. Schnöckel, I. Krossing, A. Schnepf, *Eur. J. Inorg. Chem.* **2002**, *2002*, 351.
[7] A. V. Protchenko, J. Urbano, J. A. B. Abdalla, J. Campos, D. Vidovic, A. D. Schwarz, M. P. Blake, P. Mountford, C. Jones, S. Aldridge, *Angew. Chem. Int. Ed.* **2017**, *56*, 15098.
[8] I. Krossing, A. Reisinger, *Coord. Chem. Rev.* **2006**, *250*, 2721.
[9] a) T. A. Engesser, M. R. Lichtenthaler, M. Schleep, I. Krossing, *Chem. Soc. Rev.* **2016**, *45*, 789; b) I. M. Riddlestone, A. Kraft, J. Schaefer, I. Krossing, *Angew. Chem. Int. Ed.* **2018**, *57*, 13982.
[10] M. R. Lichtenthaler, F. Stahl, D. Kratzert, L. Heidinger, E. Schleicher, J. Hamann, D. Himmel, S. Weber, I. Krossing, *Nat. Commun.* **2015**, *6*, 8288.
[11] P. Dabringhaus, A. Barthélemy, I. Krossing, *Z. Anorg. Allg. Chem.* **2021**, *647*, 1660.
[12] K. Glootz, D. Kratzert, D. Himmel, A. Kastro, Z. Yassine, T. Findeisen, I. Krossing, *Angew. Chem. Int. Ed.* **2018**, *57*, 14203.
[13] K. Glootz, D. Himmel, D. Kratzert, B. Butschke, H. Scherer, I. Krossing, *Angew. Chem. Int. Ed.* **2019**, *58*, 14162.
[14] J. M. Slattery, A. Higelin, T. Bayer, I. Krossing, *Angew. Chem. Int. Ed.* **2010**, *49*, 3228.
[15] S. Welsch, M. Bodensteiner, M. Dušek, M. Sierka, M. Scheer, *Chem. Eur. J.* **2010**, *16*, 13041.
[16] F. E. Hahn, *Chem. Rev.* **2018**, *118*, 9455.
[17] C. Shan, S. Yao, M. Driess, *Chem. Soc. Rev.* **2020**, *49*, 6733.
[18] A. Higelin, U. Sachs, S. Keller, I. Krossing, *Chem. Eur. J.* **2012**, *18*, 10029.

[19] A. Higelin, S. Keller, C. Göhringer, C. Jones, I. Krossing, *Angew. Chem. Int. Ed.* **2013**, *52*, 4941.
[20] a) T. Chu, G. I. Nikonov, *Chem. Rev.* **2018**, *118*, 3608; b) M. Zhong, S. Sinhababu, H. W. Roesky, *Dalton Trans.* **2020**, *49*, 1351.
[21] a) C. A. Tolman, *J. Am. Chem. Soc.* **1970**, *92*, 2956; b) C. A. Tolman, *Chem. Rev.* **1977**, *77*, 313.
[22] a) T. J. McNeese, S. S. Wreford, B. M. Foxman, *J. Chem. Soc., Chem. Commun.* **1978**, 500; b) J. E. Salt, G. S. Girolami, G. Wilkinson, M. Motevalli, M. Thornton-Pett, M. B. Hursthouse, *J. Chem. Soc., Dalton Trans.* **1985**, 685; c) G. S. Girolami, G. Wilkinson, A. M. R. Galas, M. Thornton-Pett, M. B. Hursthouse, *J. Chem. Soc., Dalton Trans.* **1985**, 1339; d) A. W. Kaplan, R. G. Bergman, *Organometallics* **1998**, *17*, 5072; e) J. Han, D. Coucouvanis, *Inorg. Chem.* **2002**, *41*, 2738; f) K. Venkatesan, O. Blacque, T. Fox, M. Alfonso, H. W. Schmalle, H. Berke, *Organometallics* **2004**, *23*, 4661; g) L. R. Doyle, P. J. Hill, G. G. Wildgoose, A. E. Ashley, *Dalton Trans.* **2016**, *45*, 7550.
[23] a) N. E. Miller, E. L. Muetterties, *J. Am. Chem. Soc.* **1964**, *86*, 1033; b) J. T. Leman, H. A. Roman, A. R. Barron, *J. Chem. Soc., Dalton Trans.* **1992**, 2183; c) J. Burt, W. Levason, M. E. Light, G. Reid, *Dalton Trans.* **2014**, *43*, 14600; d) P. A. Gray, J. W. Saville, K. D. Krause, N. Burford, R. McDonald, M. J. Ferguson, *Can. J. Chem.* **2017**, *95*, 346.
[24] B. Twamley, P. P. Power, *Angew. Chem. Int. Ed.* **2000**, *39*, 3500.
[25] a) N. Takagi, M. W. Schmidt, S. Nagase, *Organometallics* **2001**, *20*, 1646; b) H.-J. Himmel, H. Schnöckel, *Chem. Eur. J.* **2002**, *8*, 2397.
[26] A. Bondi, *J. Phys. Chem.* **1964**, *68*, 441.
[27] P. Pyykkö, M. Atsumi, *Chem. Eur. J.* **2009**, *15*, 186.
[28] I. Krossing, H. Brands, R. Feuerhake, S. Koenig, *J. Fluorine Chem.* **2001**, *112*, 83.
[29] A. Barthélemy and I. Krossing, unpublished results.
[30] W. M. Haynes (Ed.), *CRC handbook of chemistry and physics. A ready-reference book of chemical and physical data*, 97th ed., CRC Press, Boca Raton, London, New York, **2017**, p. 6–206.
[31] a) E. A. Carter, W. A. Goddard, *J. Phys. Chem.* **1986**, *90*, 998; b) G. Treboux, J. C. Barthelat, *J. Am. Chem. Soc.* **1993**, *115*, 4870; c) M. Driess, H. Grützmacher, *Angew. Chem. Int. Ed.* **1996**, *35*, 828; d) P. P. Power, *Chem. Rev.* **1999**, *99*, 3463.
[32] a) W. E. Lindsell, K. J. McCullough, A. J. Welch, *J. Am. Chem. Soc.* **1983**, *105*, 4487; b) A. P. Ginsberg, W. E. Lindsell, K. J. McCullough, C. R. Sprinkle, A. J. Welch, *J. Am. Chem. Soc.* **1986**, *108*, 403; c) I. Krossing, L. van Wüllen, *Chem. Eur. J.* **2002**, *8*, 700; d) S. Dürr, D. Ertler, U. Radius, *Inorg. Chem.* **2012**, *51*, 3904; e) J. W. Dube, C. M. E. Graham, C. L. B. Macdonald, Z. D. Brown, P. P. Power, P. J. Ragogna, *Chem. Eur. J.* **2014**, *20*, 6739; f) C. C. Mokhtarzadeh, A. L. Rheingold, J. S. Figueroa, *Dalton Trans.* **2016**, *45*, 14561; g) M. J. Drance, S. Wang, M. Gembicky, A. L. Rheingold, J. S. Figueroa, *Organometallics* **2020**, *39*, 3394; h) R. Grünbauer, G. Balázs, M. Scheer, *Chem. Eur. J.* **2020**, *26*, 11722; i) D. Reiter, P. Frisch, D. Wendel, F. M. Hörmann, S. Inoue, *Dalton Trans.* **2020**, *49*, 7060.
[33] G. Prabusankar, A. Doddi, C. Gemel, M. Winter, R. A. Fischer, *Inorg. Chem.* **2010**, *49*, 7976.
[34] a) A. Schmidpeter, S. Lochschmidt, W. S. Sheldrick, *Angew. Chem. Int. Ed.* **1982**, *21*, 63; b) J. A. Boon, H. L. Byers, K. B. Dillon, A. E. Goeta, D. A. Longbottom, *Heteroat. Chem.* **2000**, *11*, 226; c) E. M. Dionisi, J. F. Binder, J. H. W. LaFortune, C. L. B. Macdonald, *Dalton Trans.* **2020**, *49*, 12115.
[35] I. Krossing, *Chem. Eur. J.* **2001**, *7*, 490.

Manuscript received: May 4, 2022
Accepted manuscript online: June 13, 2022
Version of record online: July 28, 2022